

Ionic Association Effects upon Optical Electron Transfer Energetics: Studies in Water with $(\text{CN})_5\text{Fe}^{\text{II}}\text{--BPE--Fe}^{\text{III}}(\text{CN})_5^{5-}$

Robert L. Blackburn, Yuhua Dong, L. Andrew Lyon, and Joseph T. Hupp*

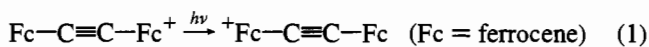
Department of Chemistry, Northwestern University, Evanston, Illinois 60208

Received April 27, 1994[⊗]

The energetics of optical electron transfer (ET) in $(\text{NC})_5\text{Fe}^{\text{III}}\text{--bis(pyridyl)ethylene--Fe}^{\text{II}}(\text{CN})_5^{5-}$ (**1**), as monitored by intervalence absorption spectroscopy, display a remarkable sensitivity to added "inert" electrolyte. With small amounts of added NaCl, CaCl₂, or LaCl₃, the optical ET (or metal-to-metal charge transfer) energy (E^{MMCT}) increases significantly. With further additions, however, it gradually decreases, ultimately approaching (for LaCl₃) the value found in the absence of added electrolyte. The unusual intervalence energy effects are interpreted in terms of stepwise ionic association: unsymmetrical species of the type $(\text{NC})_5\text{Fe}^{\text{III}}\text{--BPE--Fe}^{\text{II}}(\text{CN})_5^{5-}\cdot\text{M}^{n+}$ absorb at higher energies than symmetrical species (i.e., **1** or $\text{M}^{n+}\cdot\text{1}\cdot\text{M}^{n+}$), because of the existence of a net unfavorable thermodynamic driving force. Support for the interpretation comes from (a) site-specific probes which show that metal cations preferentially associate with the $\{\text{--Fe}^{\text{II}}(\text{CN})_5\}^{3-}$ portion of **1** and (b) calculations of E^{MMCT} (based on experimentally determined ionic association constants and localized energy shifts) which qualitatively reproduce the observed changes in intervalence energetics. Similar intervalence energy behavior is observed for $(\text{NH}_3)_5\text{--Ru}^{\text{III}}\text{--4,4'--bpy--Ru}^{\text{II}}(\text{NH}_3)_5^{2+}$ with added Na₂SO₄. This behavior is interpreted in terms of stepwise association of SO₄²⁻ with the $\{(\text{NH}_3)_5\text{Ru}^{\text{III}}\}^{3+}$ and $\{\text{--Ru}^{\text{II}}(\text{NH}_3)_5\}^{2+}$ sites, respectively, of the polycationic mixed-valence ion. Finally, we speculatively suggest that ion-pairing-induced symmetry reduction also accounts for a most unusual literature observation: the apparent dependence of E^{MMCT} for $(\text{NH}_3)_5\text{Ru}^{\text{III}}\text{--dithiaspirane--Ru}^{\text{II}}(\text{NH}_3)_5^{5+}$ on the identity and formal potential of the oxidant used to prepare the ion from the 4+ form.

Introduction

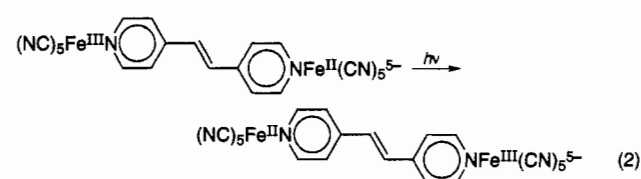
"Inert" electrolytes can exert profound effects—both favorable and unfavorable—upon the kinetics of molecule-based electron transfer processes.¹ Existing studies suggest a multiplicity of causes,¹ ranging from simple Coulombic (Debye–Huckel type) precursor formation effects to more complex activation barrier effects, electronic effects, and (perhaps) dynamical effects. In principle, the barrier effects can be separated from all other effects by measuring directly the energy cost for optical electron transfer in covalently linked donor–acceptor ("mixed-valency") systems, e.g.²



Indeed, we³ and others^{4–6} have shown (via optical ET) that such effects can be quite substantial for numerous positively charged systems, including the biferrocene monocation,³ the acetylene-bridged biferrocene monocation (eq 1),⁴ a dithiaspirane-bridged decaamminediruthenium complex (5+ charge),⁵ and various

asymmetrically coordinated diruthenium complexes (4+ charge).⁶ For each of these systems, addition of "inert" electrolyte is accompanied by monotonic increases in optical ET barrier height as demonstrated directly by blue shifts in intervalence absorption maxima. Although the experimental observations for the various systems are at least superficially similar,⁷ the interpretations are quite diverse; they include (a) ion aggregation,^{3b} (b) contact ion pairing and redox asymmetry,³ (c) specific donor (anion)/acceptor (metal complex) interactions,⁸ (d) ionic atmosphere reorganization,⁹ and (e) less specific ionic strength effects.⁵

We now wish to report findings for an anionic mixed-valence system. The species chosen was a bis(pyridyl)ethylene-bridged decacyanodiruthenium complex (**1**)—a system that Ludi and co-workers had previously shown to be sufficiently strongly electronically interacting to exhibit an easily observable optical intervalence (i.e., intramolecular electron transfer) transition:¹⁰



We reasoned that, with an overall 5– charge, complex **1** would interact readily with small, monoatomic cations of various charges. We further reasoned, however, that the largely

- [⊗] Abstract published in *Advance ACS Abstracts*, September 1, 1994.
- (1) Representative work: (a) Brown, G. M.; Sutin, N. *J. Am. Chem. Soc.* **1979**, *101*, 883. (b) Bruhn, H.; Nigam, S.; Holzwarth, J. F. *Faraday Discuss. Chem. Soc.* **1982**, *74*, 129. (c) Wherland, S.; Gray, H. In *Biological Aspects of Inorganic Chemistry*; Addison, A. W., Ed.; Wiley Interscience: New York, 1977. (d) Borchardt, D.; Wherland, S. *Inorg. Chem.* **1984**, *23*, 2537. (e) Szwarc, M. *Acc. Chem. Res.* **1972**, *5*, 169. (f) Szwarc, M. *Ions and Ion Pairs in Organic Reactions*; John Wiley and Sons: New York, 1975; Vol. 2, Chapter 1 and references therein.
- (2) For a review, see: Creutz, C. *Prog. Inorg. Chem.* **1983**, *30*, 1.
- (3) (a) Blackburn, R. L.; Hupp, J. T. *Chem. Phys. Lett.* **1988**, *150*, 399. (b) Blackburn, R. L.; Hupp, J. T. *J. Phys. Chem.* **1990**, *94*, 1788.
- (4) (a) Hammack, W. S.; Drickamer, H. G.; Lowery, M. D.; Hendrickson, D. N. *Chem. Phys. Lett.* **1986**, *132*, 231. (b) Lowery, M. D.; Hammack, W. S.; Drickamer, H. G.; Hendrickson, D. N. *J. Am. Chem. Soc.* **1989**, *111*, 8019.
- (5) (a) Lewis, N. A.; Yaw, O. S. *J. Am. Chem. Soc.* **1988**, *110*, 2307. (b) Lewis, N. A.; Yaw, O. S.; Purcell, W. L. *Inorg. Chem.* **1989**, *28*, 3796. (c) Lewis, N. A.; Yaw, O. S. *J. Am. Chem. Soc.* **1989**, *111*, 7624.
- (6) Chang, J. P.; Fung, E. Y.; Curtis, J. C. *Inorg. Chem.* **1986**, *25*, 4233.

- (7) On the other hand, there are real experimental differences: Our studies of reaction 1 showed that discrete ion-pairing and ion-tripling interactions exist,³ while studies by Hendrickson and co-workers of the biferrocene monocation showed that more complex ionic aggregation or association effects can exist.^{4b}
- (8) Curtis, J. C.; Sullivan, B. P.; Meyer, T. J. *Inorg. Chem.* **1983**, *22*, 224.
- (9) Kuznetsov, A. M.; Phelps, D. K.; Weaver, M. J. *Int. J. Chem. Kinet.* **1990**, *22*, 815.
- (10) Felix, F.; Ludi, A. *Inorg. Chem.* **1978**, *17*, 1782.

inflexible bis(pyridyl)ethylene (BPE) bridge would configure the redox centers in a sufficiently isolated fashion geometrically (ca. 14 Å metal-metal separation) that they would interact with the surrounding electrolyte components more or less independently. In selecting this target, we additionally noted the availability of literature data for the association of the $(\text{NC})_5\text{Fe}^{\text{III}}\text{L}^{2-}$ fragment with simple cations¹¹ and the likely utility of an intense metal-to-ligand charge transfer (MLCT) transition as a specific marker for interactions with the $\text{LFe}^{\text{II}}(\text{CN})_5^{3-}$ fragment.¹²

As shown below, complex 1 indeed does interact with simple cations (including H^+) in water as solvent. At low electrolyte concentrations, the interactions are manifest—as in previous studies^{3–6}—as an increase in optical ET barrier height. At higher concentrations, however, the barrier height *decreases*, ultimately approaching the value found without electrolyte perturbation. Additionally, we observe that the magnitude of the complex optical effect increases, as one might expect, as the charge of the electrolyte cation increases. Interestingly, the observed barrier effects are reminiscent of earlier studies of second-sphere interactions between $(\text{NH}_3)_5\text{Ru}^{\text{II}}-4,4'$ -bipyridine- $\text{Ru}^{\text{III}}(\text{NH}_3)_5^{5+}$ (2) and various crown ethers—where oxidation-state-sensitive, stepwise binding was encountered.^{13,14} We find that the experiments here can be understood in a related fashion by considering the optical energetic consequences of stepwise ion-pairing interactions. Finally, we find evidence for a similar barrier effect when 2 is confronted with a dianion-containing electrolyte solution. This observation seems to shed light on some otherwise puzzling findings for a related dithiaspirane-bridged system (for example, an unprecedented chemical oxidant dependence of the optical barrier to electron transfer^{5c}).

Experimental Section

Materials. The starting reagents $\text{Na}_2\text{NH}_4[\text{Fe}(\text{CN})_5(\text{NH}_3)] \cdot 2\text{H}_2\text{O}$, *trans*-1,2-bis(4-pyridyl)ethylene (BPE), 4-(dimethylamino)pyridine (dmap), and 4,4'-bipyridine (4,4'-bpy) were obtained from Aldrich and were used without further purification. Analytical grade (or better) salts were obtained from Aldrich (LaCl_3 and CaCl_2) and Mallinckrodt (NaCl). Solutions of the first two were standardized by EDTA titration.¹⁵ All visible-region experiments were carried out with water from a Millipore purification system. In order to enhance solvent transparency, measurements in the near-infrared were made in D_2O solutions.

Metal Complexes. $\text{Na}_4(\text{NH}_4)_2(\text{NC})_5\text{Fe}(\text{BPE})\text{Fe}(\text{CN})_5$ was prepared essentially as described by Felix and Ludi.¹⁰ Purification (probable removal of monomeric species) was achieved via primitive size exclusion chromatography (Bio-Gel P-2 200-400 mesh, Bio-Rad Laboratories) with water as eluent. (In subsequent preparations, we found that the chromatography step could be omitted by more carefully avoiding exposure of the dissolved product to light.) The mixed-valence ion, 1, was generated *in situ* by adding increments of Br_2 vapor while the metal-to-metal charge transfer band was monitored. $\text{Na}_2(\text{NH}_4)[(\text{NC})_5\text{Fe}(\text{dmap})]$ and $[(\text{NH}_3)_5\text{Ru}-4,4'\text{-bpy}-\text{Ru}(\text{NH}_3)_5](\text{PF}_6)_4$ were also prepared and purified by literature methods.^{11,16} For use in water, the latter was converted to the chloride salt. The mixed-valence form, 2, was generated *in situ* by using Br_2 vapor as oxidant.

Measurements. All visible and near-infrared (near-IR) measurements were obtained by using a matched set of 1 cm cells in an OLIS-

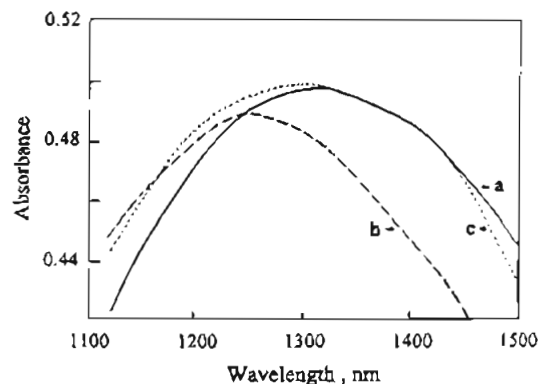


Figure 1. Intervalence absorption spectra for $(\text{NC})_5\text{Fe}^{\text{III}}\text{-BPE-Fe}^{\text{II}}(\text{CN})_5^{3-}$ in D_2O : (a) without added electrolyte; (b) with 0.020 M LaCl_3 ; (c) with 2.02 M LaCl_3 .

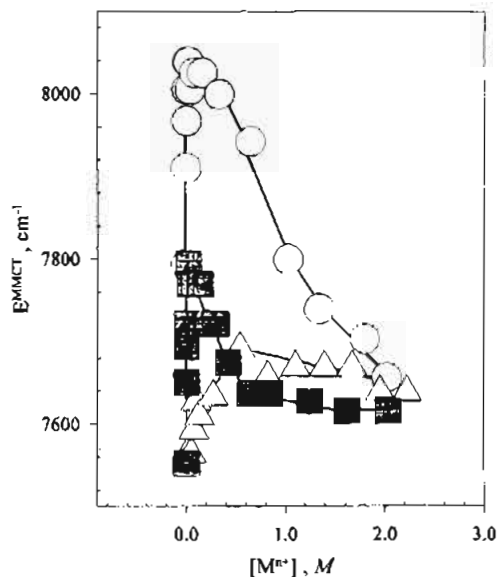


Figure 2. Dependence of the intervalence charge transfer energy maximum for reaction 2 (in D_2O) on concentration of added LaCl_3 (O), CaCl_2 (■), and NaCl (Δ).

modified Cary 14 spectrometer. Absorbance peak energies could be reproducibly determined to within $\pm 50 \text{ cm}^{-1}$ in the visible region and $\pm 65 \text{ cm}^{-1}$ in the near-IR. Initial MMCT measurements were made without added electrolyte. Dilutions were made until the absorption energy ceased shifting. We took this as evidence that self-association effects (chromophore + counterion) had been eliminated. Subsequently, a chromophore (1) concentration of 0.6 mM was employed in the near-IR, while a concentration of 0.4 mM was used in the visible region.

Because of the possibility for protonation of 1 (see below), particular attention was given to the solution pH. In most electrolyte-containing solutions, the pH was 6 or greater (without added buffers). One experiment with LaCl_3 was performed with 0.03 M added sodium acetate/acetic acid buffer (pH = 6.5), to confirm that La^{3+} hydrolysis was not biasing the investigation. Additional experiments in the pH = 2–7 range were carried out at low ionic strength by using acetate buffers again or added HCl. pH's were measured with a glass combination electrode that had been calibrated with several known buffer solutions.

Analysis. Equilibrium constants and associated standard errors were obtained from nonlinear least squares fits of experimental data (χ^2 minimization) by using Kaleidagraph (Abelbeck Software). (Nearly identical results were obtained with SigmaPlot (Jandel Scientific)—a related nonlinear least squares program featuring a slightly different fitting algorithm.)

Results

Figure 1 shows absorption spectra (peak region only) for transition 2 in D_2O , without added electrolyte, with 0.020 M

- (11) Warner, L. W.; Hoq, M. F.; Myser, T. K.; Henderson, W. W.; Shepherd, R. E. *Inorg. Chem.* **1986**, *25*, 1911.
- (12) See, for example: Moya, M. L.; Rodriguez, A.; Sanchez, F. *Inorg. Chim. Acta* **1991**, *188*, 185; **1992**, *197*, 227.
- (13) (a) Hupp, J. T.; Dong, Y.; Todd, M. D. *Inorg. Chem.* **1991**, *30*, 4687. (b) Todd, M. D.; Dong, Y.; Horney, J.; Hupp, J. T. *Inorg. Chem.* **1993**, *32*, 2001.
- (14) See also: (a) Weydert, J.; Hupp, J. T. *Inorg. Chem.* **1987**, *26*, 2657. (b) Roberts, J. A.; Hupp, J. T. *Inorg. Chem.* **1992**, *31*, 1540. (c) Dong, Y.; Hupp, J. T.; Yoon, D. I. *J. Am. Chem. Soc.* **1993**, *115*, 4379.
- (15) Yalman, R. G.; Bruegemann, W.; Baker, P. T.; Garn, S. M. *Anal. Chem.* **1959**, *31*, 1230.
- (16) Blackburn, R. L.; Hupp, J. T. *J. Phys. Chem.* **1988**, *92*, 2817.

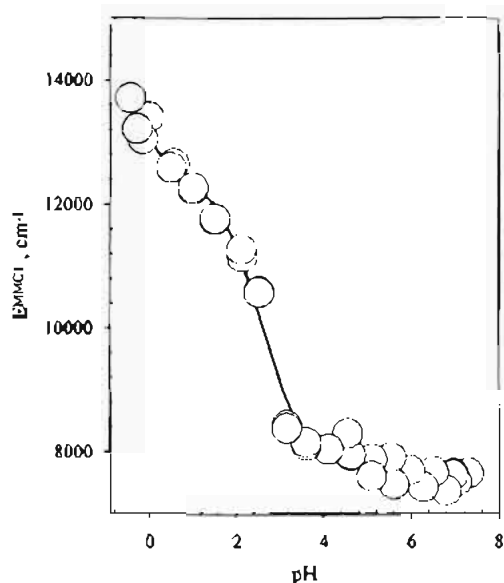
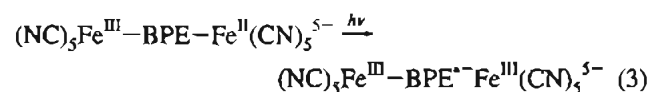


Figure 3. Dependence of the intervalence charge transfer energy maximum for reaction 3 on pH.

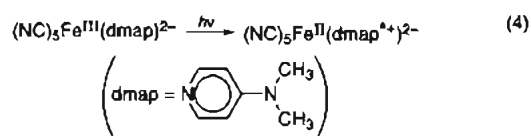
La^{3+} and, finally, with 2.02 M La^{3+} (as the chloride salt). The unusual aspect, shown in more detail in Figure 2, is the sharp shift of the MMCT absorbance maximum to higher energy with modestly increasing electrolyte concentration, coupled with shifts back toward the initial energy as $[\text{La}^{3+}]$ is further increased. Essentially the same pattern (albeit, with smaller energy shifts) is observed with added Ca^{2+} (Figure 2)—while only limited hints of similar behavior are seen with added Na^+ (Figure 2). As shown in Figure 3, blue shifts in MMCT energy (but apparently not red shifts) can also be induced by varying the buffered activity of H^+ .

The behavior with both La^{3+} and Ca^{2+} is clearly suggestive of multiple Coulombic or other interactions, perhaps occurring at multiple sites. To simplify the investigation, we also examined, therefore, electronic transitions involving only a single pentacyanoiron center. In Figure 4, the energy for metal-to-ligand (Fe^{II} -to-BPE) charge transfer in **1** (E^{MLCT} ; eq 3) is



plotted versus added electrolyte cation concentration. In principle, this transition should offer a highly localized probe of environmental effects. In any case, the observed energy increases monotonically as the cation concentration increases—with the effects again ordered as $\text{La}^{3+} > \text{Ca}^{2+} > \text{Na}^+$.

Related transitions involving the bridging ligand and Fe^{III} should exist (i.e. ligand-to-metal charge transfer (LMCT)). These, of course, should also function as localized probes, but at the opposite end of the mixed-valence ion. Unfortunately, they are obscured by other transitions (presumably intraligand transitions) in the UV region. As a surrogate for the $(\text{NC})_5\text{Fe}^{\text{III}}\text{L}$ fragment of **1**, therefore, we have examined LMCT in $(\text{NC})_5\text{Fe}^{\text{III}}(\text{dmap})^{2-}$:



As shown in Figure 5, E^{LMCT} monotonically decreases with

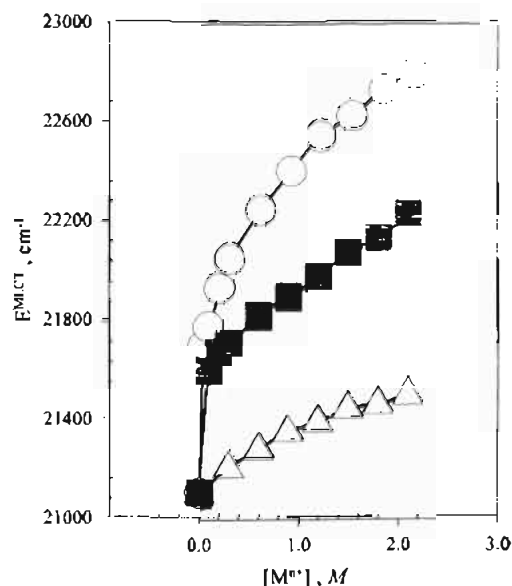


Figure 4. Dependence of the metal-to-ligand charge transfer energy maximum for **1** on concentration of added LaCl_3 (O), CaCl_2 (■), and NaCl (Δ).

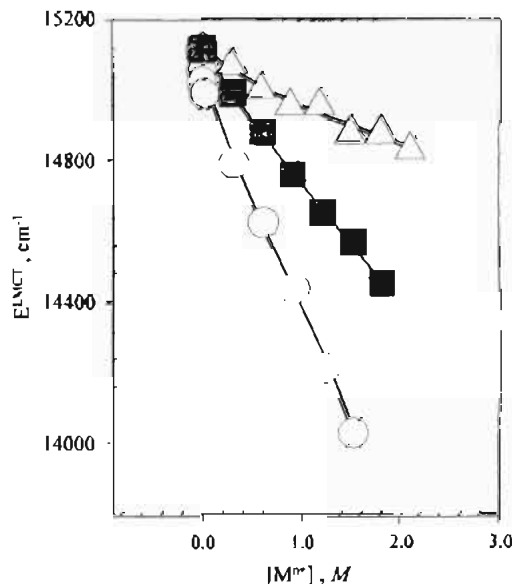
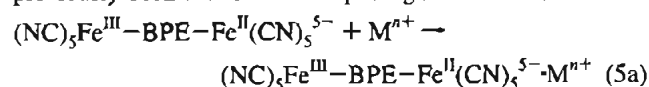


Figure 5. Dependence of the ligand-to-metal charge transfer energy maximum for $(\text{NC})_5\text{Fe}(\text{dmap})^{2-}$ on concentration of added LaCl_3 (O), CaCl_2 (■), and NaCl (Δ).

increasing cation concentration—with the absolute energy shifts ordered as $\text{La}^{3+} > \text{Ca}^{2+} > \text{Na}^+$.

Discussion

Cation Effects: Monomeric Species. The range of electrolyte effects in Figures 1–5 (obtained for the most part with a common anion) is clearly suggestive of specific cation effects. The most striking of these are the “bidirectional” energy effects observed for metal-to-metal charge transfer (eq 1; Figures 1 and 2). We prefer to focus initially, however, on the single-site MLCT and LMCT transitions. Cation effects here have previously been ascribed to ion-pairing interactions,^{11,12} i.e.



$\text{M}^{n+} + (\text{NC})_5\text{Fe}^{\text{III}}(\text{dmap})^{2-} \rightarrow \text{M}^{n+}\cdot(\text{NC})_5\text{Fe}^{\text{III}}(\text{dmap})^{2-}$ (6)
More specifically, for the LMCT transition, the shifts to lower energy have been explained in terms of significant ground state

electrostatic interactions between $(\text{NC})_5\text{Fe}^{\text{III}}\text{L}^{2-}$ and M^{n+} , together with enhanced interactions between $(\text{NC})_5\text{Fe}^{\text{II}}(\text{L}^+)^{2-}$ (i.e. the LMCT excited state) and M^{n+} —where M^{n+} in both cases is presumed to interact with one or more of the negatively charged cyanide ligands. (These ligands, of course, should be more completely negatively charged when bound to Fe^{II} than to Fe^{III} .) In any case, preferential stabilization of Fe^{II} should lead to compression of the upper-state/lower-state energy gap and a red shift in E^{LMCT} , as indeed seen experimentally. A related argument leads to the prediction of a blue shift for the MLCT transition following ionic association.

In principle, the observed shifts can be used to quantify (at least approximately) the ion-pairing thermodynamics. For example, if only two chromophoric species are present (paired and unpaired complexes), if their extinction coefficients are similar, and if the difference in their absorption energies is small compared with the widths of the individual absorption bands, then the observed transition energy at any finite cation concentration can be taken simply as the population-weighted arithmetic mean of the energies for the paired and unpaired species. A series of such energies can then be fit, as follows, to extract an ion-pairing constant (K_{IP}):

$$E = E_{\text{init}} + \{K_{\text{IP}}\gamma[\text{M}^{n+}]\Delta E\}/\{1 + K_{\text{IP}}\gamma[\text{M}^{n+}]\} \quad (7)$$

In eq 7, E_{init} is the transition energy in the absence of ion pairing, ΔE is the difference between E_{init} and E when ion pairing is complete, and γ is an activity coefficient for M^{n+} . (Strictly speaking, the equation also should contain a ratio of activity coefficients for the free and ion-paired pentacyanoiron complexes. Both for simplicity and for lack of detailed information, we assume that the ratio is unity at all ionic strengths.)

The E^{MLCT} vs $[\text{M}^{n+}]$ data shown in Figure 4 exhibit, as least qualitatively, the curved, asymptotic shape predicted by eq 7. A nonlinear least squares fit for $\text{M}^{n+} = \text{La}^{3+}$ yields $K_{\text{IP}} = 5 \pm 1 \text{ M}^{-1}$ and $\Delta E = 1690 \pm 100 \text{ cm}^{-1}$, for reaction 5a. Correction of the plot using published activity coefficients (see Figure 6)^{17,18} significantly enhances the curvature and yields $K_{\text{IP}} = 20 \pm 3 \text{ M}^{-1}$ and $\Delta E = 1630 \pm 50 \text{ cm}^{-1}$. Related plots for $\text{M}^{n+} = \text{Ca}^{2+}$ and Na^+ yield activity-coefficient-corrected ion-pairing constants of 11 ± 4 and $0.9 \pm 0.1 \text{ M}^{-1}$, respectively, and energy shifts of 1060 ± 50 and $740 \pm 50 \text{ cm}^{-1}$; their full significance is unclear, however, since multiple ionic association equilibria may well exist.

A similar analysis for reaction 6 (based on LMCT excitation of $(\text{NC})_5\text{Fe}^{\text{III}}(\text{dmap})^{2-}$ (eq 4) and using the γ values in Figure 6) yields $K_{\text{IP}}(\text{La}^{3+}) = 3 \pm 0.6 \text{ M}^{-1}$ and $\Delta E(\text{La}^{3+}) = -1480 \pm 130 \text{ cm}^{-1}$. Estimated K_{IP} values (activity corrected) for Ca^{2+} and Na^+ are 0.9 ± 0.1 and $0.4 \pm 0.2 \text{ M}^{-1}$; ΔE values are -1260 ± 70 and $-770 \pm 280 \text{ cm}^{-1}$, respectively. Comparison of these K_{IP} values to those for reaction 5 ($-\text{Fe}^{\text{II}}(\text{CN})_5^{3-}$, M^{n+}) show the latter to be significantly larger—consistent with a more negative metal complex charge and a larger anion/cation change product. The ion-pairing constants also becomes larger (for both reactions) as the charge of the free metal cation (M^{n+}) increases. Turning to the energy effects, these likewise increase as the

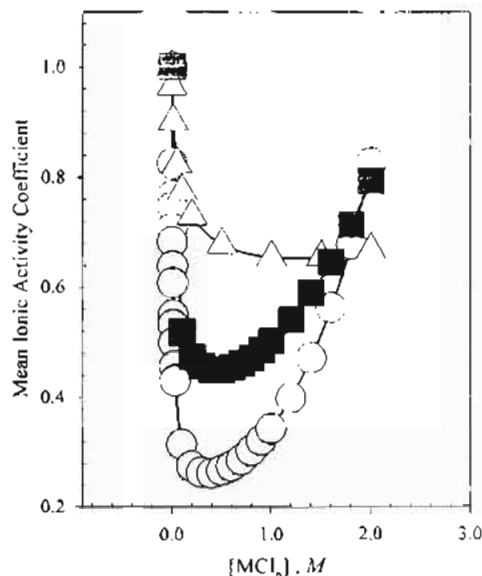
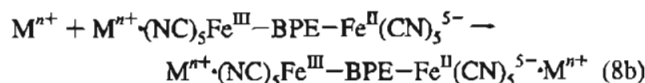
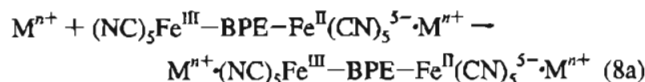
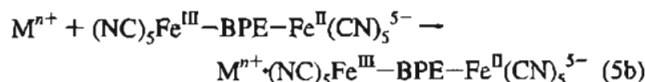


Figure 6. Mean ionic activity coefficients vs molar concentration for aqueous LaCl_3 (O), CaCl_2 (■), and NaCl (Δ) (data taken from ref 18).

charge of the free metal ion increases. Approximate scaling of the energy effects with charge is not unexpected: neglecting Franck–Condon effects,¹⁹ ΔE should provide a measure of the differential stabilization (by cation pairing) of $\{(\text{NC})_5\text{Fe}^{\text{II}}-\}^{3-}$ versus $\{(\text{NC})_5\text{Fe}^{\text{III}}-\}^{2-}$. One further observation of significance is the approximate quantitative agreement (for a given M^{n+}) of ΔE for MLCT excitation (eq 3) with $-\Delta E$ for LMCT excitation (eq 4). Since both processes effectively connect a $\{(\text{NC})_5\text{Fe}^{\text{II}}-\}^{3-}$ -containing state with a $\{(\text{NC})_5\text{Fe}^{\text{III}}-\}^{2-}$ -containing state, there is an approximate Coulombic basis for similarity in absolute ΔE values. (Recall again that ΔE should primarily be a measure of the differential electrostatic stabilization of the two states by cation pairing.)

Cation Effects: Dimeric Species. The substantial difference in ion-pairing constants for $(\text{NC})_5\text{Fe}^{\text{III}}\text{L}^{2-}$ versus $\text{LFe}^{\text{II}}(\text{CN})_5^{3-}$ has interesting consequences for the mixed-valence complex, 1. Depending on the M^{n+} concentration, this species could exist in any of four forms interconnected by the ion-pairing equilibria shown in eq 5a (above) and eqs 5b, 8a, and 8b. Assuming (a)



that K_{IP} for eqs 5b and 8a can be adequately approximated by K_{IP} for eq 6 and (b) that K_{IP} for eq 8b equals K_{IP} for eq 5a, the fractions α_0 , α_1 , α_2 , and α_3 of $(\text{NC})_5\text{Fe}^{\text{III}}-\text{BPE}-\text{Fe}^{\text{II}}(\text{CN})_5^{5-}$, $\text{M}^{n+}\cdot(\text{NC})_5\text{Fe}^{\text{III}}-\text{BPE}-\text{Fe}^{\text{II}}(\text{CN})_5^{5-}$, $(\text{NC})_5\text{Fe}^{\text{III}}-\text{BPE}-\text{Fe}^{\text{II}}(\text{CN})_5^{5-}\cdot\text{M}^{n+}$, and $\text{M}^{n+}\cdot(\text{NC})_5\text{Fe}^{\text{III}}-\text{BPE}-\text{Fe}^{\text{II}}(\text{CN})_5^{5-}\cdot\text{M}^{n+}$, respectively, can be calculated at any M^{n+} activity (or concentration). Figure 7, for example, shows plots of α_i as a function of La^{3+} concentration.

If the MMCT extinction coefficients are similar for each of the four mixed-valence forms, then the α_i values can subse-

(17) Unfortunately, the single-ion activity coefficients (γ) required for eq 7 are thermodynamically inaccessible. While these can, in principle, be calculated (for example, from extended Debye–Hückel theory or more sophisticated theories), the reliability of such calculations is suspect at both intermediate and high ionic strengths. As a compromise, we have chosen to use experimentally determined,¹⁸ mean ionic activity coefficients (γ^\pm).

(18) (a) Robinson, R. A.; Stokes, R. H. *Electrolyte Solutions*, 2nd ed.; Butterworths: New York, 1970. (b) Lobo, V. M. M. *Electrolyte Solutions: Literature Data on Thermodynamic and Transport Properties*; Columbia Press: Coimbra, Portugal, 1984.

(19) Our primitive argument also neglects energy effects due to upper-state interactions between M^{n+} and L^+ or L^- .

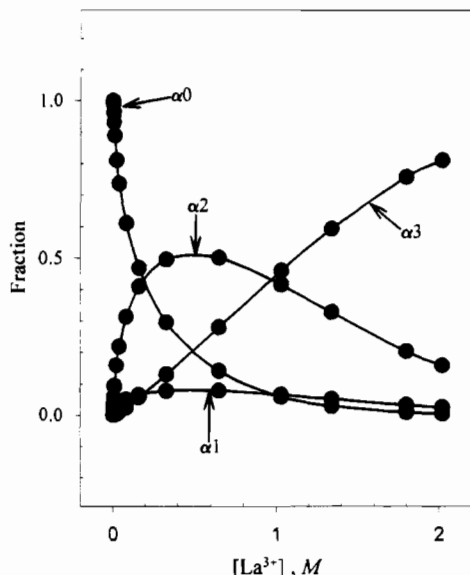


Figure 7. Calculated fractions of **1** in various forms (see text), as a function of La^{3+} concentration. Key to fractions: α_0 , $(\text{NC})_5\text{Fe}^{\text{III}}-\text{BPE}-\text{Fe}^{\text{II}}(\text{CN})_5^{5-}$; α_1 , $\text{La}^{3+}(\text{NC})_5\text{Fe}^{\text{III}}-\text{BPE}-\text{Fe}^{\text{II}}(\text{CN})_5^{5-}$; α_2 , $(\text{NC})_5\text{Fe}^{\text{III}}-\text{BPE}-\text{Fe}^{\text{II}}(\text{CN})_5^{5-}\cdot\text{La}^{3+}$; α_3 , $\text{La}^{3+}(\text{NC})_5\text{Fe}^{\text{III}}-\text{BPE}-\text{Fe}^{\text{II}}(\text{CN})_5^{5-}\cdot\text{La}^{3+}$.

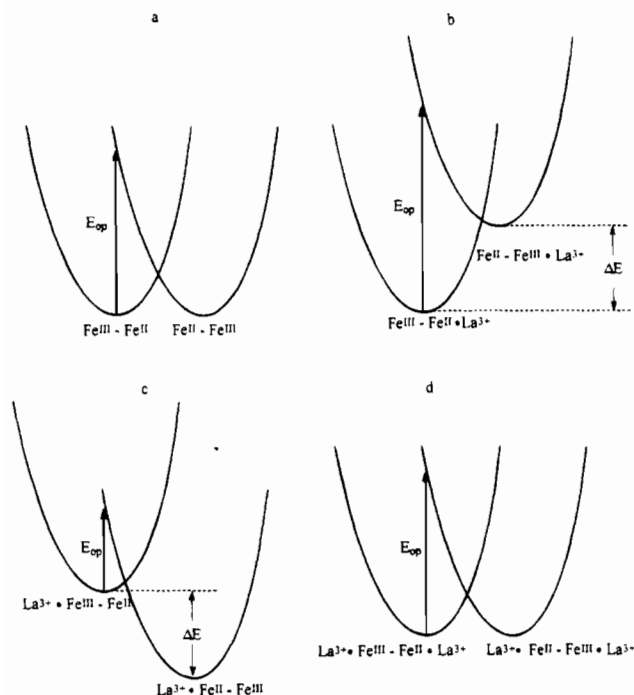


Figure 8. Energy diagrams for intervalence electron transfer in (a) $(\text{NC})_5\text{Fe}^{\text{III}}-\text{BPE}-\text{Fe}^{\text{II}}(\text{CN})_5^{5-}$, (b) $(\text{NC})_5\text{Fe}^{\text{III}}-\text{BPE}-\text{Fe}^{\text{II}}(\text{CN})_5^{5-}\cdot\text{La}^{3+}$, (c) $\text{La}^{3+}(\text{NC})_5\text{Fe}^{\text{III}}-\text{BPE}-\text{Fe}^{\text{II}}(\text{CN})_5^{5-}$, and (d) $\text{La}^{3+}(\text{NC})_5\text{Fe}^{\text{III}}-\text{BPE}-\text{Fe}^{\text{II}}(\text{CN})_5^{5-}\cdot\text{La}^{3+}$.

quently be used to calculate a composite MMCT absorption energy at any M^{n+} activity:

$$E^{\text{MMCT}} = \alpha_0 E_0 + \alpha_1 E_1 + \alpha_2 E_2 + \alpha_3 E_3 \quad (9)$$

In applying eq 9, we have assumed (see Figure 8) that E_3 equals E_0 , i.e. that double ion pairing does not significantly affect the reorganization energy (λ) for intervalence ET. (Note that E_{op} should (approximately²⁰) equal λ in symmetrical mixed-valence systems,^{2,21} such as the free and doubly ion-paired systems.) For $(\text{NC})_5\text{Fe}^{\text{III}}-\text{BPE}-\text{Fe}^{\text{II}}(\text{CN})_5^{5-}\cdot\text{M}^{n+}$, on the other hand, ion pairing (a) reduces the overall symmetry, (b) renders the initial and final intervalence states structurally inequivalent, and (c)

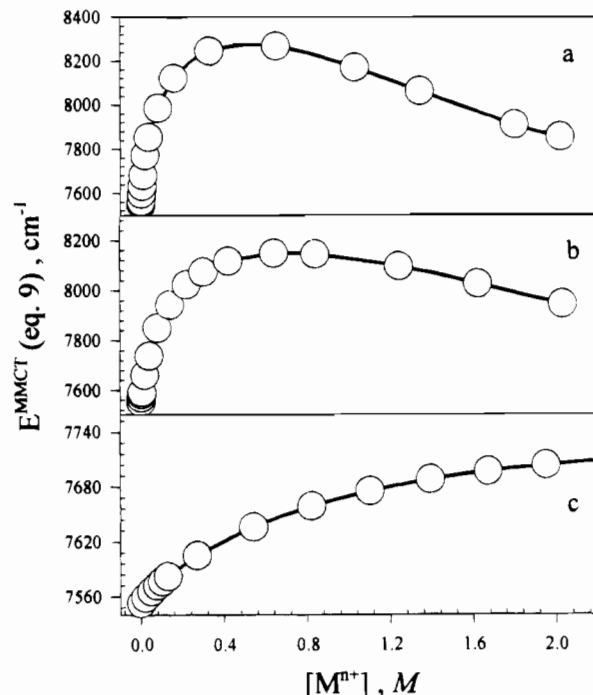


Figure 9. Calculated values of E^{MMCT} for $(\text{NC})_5\text{Fe}^{\text{III}}-\text{BPE}-\text{Fe}^{\text{II}}(\text{CN})_5^{5-}$ (see eq 9 and text) as a function of added electrolyte concentration: (a) LaCl_3 ; (b) CaCl_2 ; (c) NaCl .

adds to the overall optical energy a term (ΔE) that reflects the corresponding *energetic* inequivalence of the vibrationally and librally relaxed initial and final states (see Figure 8).^{3,4b} Thus, E_2 should equal $E_0 + \Delta E$. In addition, if ΔE originates exclusively from preferential electrostatic stabilization (by M^{n+}) of $\{-\text{Fe}^{\text{II}}(\text{CN})_5\}^{3-}$ (intervalence ground state) relative to $\{(\text{NC})_5\text{Fe}^{\text{III}}-\}^{2-}$ (intervalence excited state), then its value should be given approximately by the limiting MLCT energy shifts discussed above. For $\text{M}^{n+}(\text{NC})_5\text{Fe}^{\text{III}}-\text{BPE}-\text{Fe}^{\text{II}}(\text{CN})_5^{5-}$, the symmetry is similarly reduced. Now, however, ion pairing preferentially stabilizes the intervalence *excited* state. Consequently, E_1 should equal E_0 minus ΔE (where ΔE again can be equated with the limiting MLCT energy shift or, equivalently, with the negative of the LMCT energy shifts).

Figure 9a presents composite MMCT values (eq 9) for $\text{M}^{n+} = \text{La}^{3+}$ (with energies plotted versus concentration to facilitate comparison with Figure 2). Reasonably good qualitative agreement with direct MMCT measurements exists. For example, the calculated intervalence energy clearly increases significantly and then decreases with increasing La^{3+} activity. At a more quantitative level, however, the agreement is less satisfactory: Equation 9 and the data in Figure 7 slightly overestimate the magnitude of the positive energy shift while underestimating the sharpness of the shift. Indeed, to reproduce the data in Figure 2 via the composite energy calculation, significantly higher apparent K_{IP} values (eqs 5 and 8) would be required.

(20) Strictly speaking, vertical energy differences in diagrams such as Figure 8 are most appropriately identified with maxima in plots of (absorbance/energy) vs energy, rather than simply absorbance vs energy. (See, for example: Reimers, J. R.; Hush, N. S. *Inorg. Chem.* **1990**, *29*, 3686.) Even with this correction, observed E^{MMCT} values for symmetrical systems will differ from λ if spin-orbit coupling (small for iron) and/or ligand field asymmetry (perhaps larger) removes the degeneracy of the $d\pi(\text{metal})$ levels and if intervalence transitions to the available spin-orbit excited states have significant oscillator strength. (See: Kober; et al. *J. Am. Chem. Soc.* **1985**, *105*, 4303; Hupp; Meyer. *Inorg. Chem.* **1987**, *26*, 2332.)

(21) Hush, N. S. *Trans. Faraday Soc.* **1961**, *57*, 557.

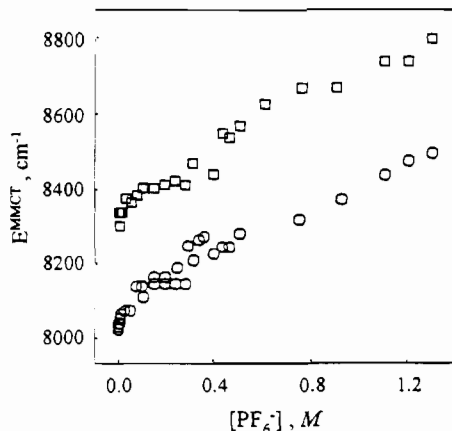


Figure 10. Dependence of E^{MMCT} for $(\text{NH}_3)_5\text{Ru}^{\text{III}}-4,4'\text{-bpy}-\text{Ru}^{\text{II}}-(\text{NH}_3)_5^{5+}$ on concentration of added $(\text{TEA})\text{PF}_6$ in DMSO (○) and DMF (□).

For $M^{n+} = \text{Ca}^{2+}$, qualitative agreement again exists between the calculated (composite) intervalence energies (Figure 9b) and the experimental energies (Figure 2), in the sense that both display an increase followed by a decrease as the cation concentration is made progressively higher. The magnitude of the energy shift, however, is overestimated by the calculation (by ca. 2-fold), as is the concentration where the energy maximizes (by several-fold). Finally, for $M^{n+} = \text{Na}^+$, the composite calculation does a fair job of reproducing the observed overall dependence of E^{MMCT} on added cation concentration but fails to reproduce the apparent energy decrease at the highest concentrations. Again, higher apparent K_{IP} values would be required in order to reproduce the direct measurements.

Despite the lack of exact agreement, we view the qualitative similarities between direct MMCT measurements (Figure 2) and the results of eq 9 (Figure 9) as compelling evidence for the approximate validity of the sequential ion-pairing model in describing the unusual intervalence energetics of **1**. Residual quantitative differences could be due to (a) the use of $(\text{NC})_5\text{Fe}^{\text{III}}(\text{dmap})^{2-}$ as a surrogate for the pentacyanoiron(III) site of **1**, (b) neglect of higher order ionic association equilibria, (c) the use of mean ionic activity coefficients (Figure 6)¹⁷ rather than single ion activity coefficients (M^{n+}) in determining ion-pairing constants, and/or (d) neglect of non-specific, ionic atmosphere reorganization effects.⁹ Lack of a major role for (d) seems to be indicated by the approximate numerical agreement between E^{MMCT} without added electrolyte (ionic strength ≈ 0) and E^{MMCT} with 2.02 M LaCl_3 (ionic strength = 10 M). The effects of c, on the other hand, should largely cancel if consistency is maintained in determining apparent K_{IP} values and in subsequently comparing experiment and calculation. A related, but more subtle, source of error may be the representation of each ion-pairing step by a completely ionic-strength-independent equilibrium constant. Clearly, the K_{IP} value for pairing **1** with La^{3+} (the predominant cation form at low ionic strength) will differ from the value for pairing **1** with $(\text{La}\cdot\text{Cl})^{2+}$ (presumably the predominant cation form at intermediate ionic strengths)—yet our analysis overlooks the difference. It should be noted that while empirically determined mean ionic activity corrections¹⁸ implicitly account for a portion of the effect (by effectively lowering the M^{n+} activity when $M^{n+}\cdot\text{Cl}^-$ association occurs), they cannot fully correct for K_{IP} variations in eqs 5 and 8.

pH Effects. In view of the discussion above, it is tempting to ascribe the observed pH dependence of intervalence electron transfer in **1** (Figure 3) to selective protonation of $(\text{NC})_5\text{Fe}^{\text{II}}-$. The limiting blue shift at low pH's (lower than examined here)

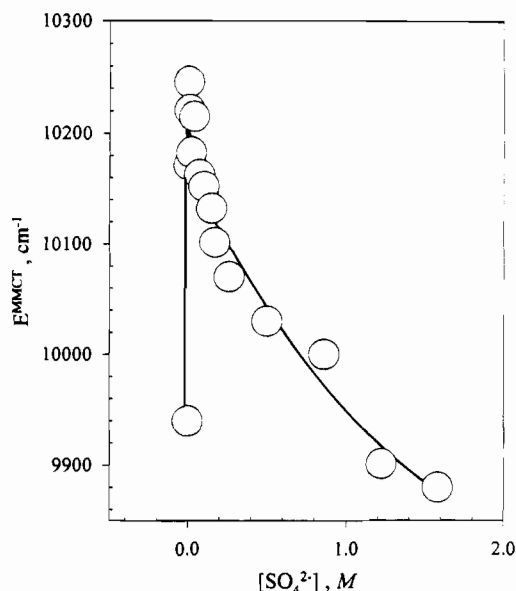
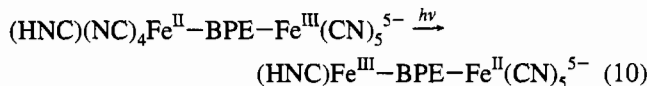


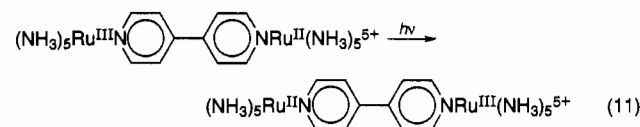
Figure 11. Dependence of E^{MMCT} for $(\text{NH}_3)_5\text{Ru}^{\text{III}}-4,4'\text{-bpy}-\text{Ru}^{\text{II}}-(\text{NH}_3)_5^{5+}$ on concentration of added Na_2SO_4 in D_2O as solvent.

would represent the extra energy associated with structural and redox symmetry in the reaction



Lack of a red shift is interpreted simply as an inability to examine the reaction at pH's below the $\text{p}K_{\text{b}}$ of the $-\text{Fe}^{\text{III}}(\text{CN})_5$ fragment.

Anion Effects. In view of the unusual "specific cation" effects (above) for intervalence transfer in polyanionic complexes, we reasoned that specific *anion* effects should exist for *polycationic* complexes. Figure 10 shows intervalence energy data for a polycationic reaction (eq 11) as a function of added



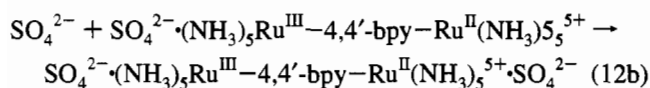
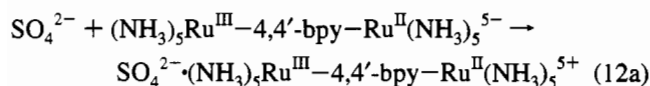
tetrabutylammonium hexafluorophosphate ($\text{TBA}^+\text{PF}_6^-$) concentration in both dimethyl sulfoxide (lower curve) and dimethylformamide (upper curve) as solvent. Figure 11 shows data for the same reaction (eq 11), but now as a function of added Na_2SO_4 concentration in water as solvent.²²

The monotonic energy increases found in DMSO and DMF are highly reminiscent of electrolyte effects reported by Lewis and co-workers for intervalence transfer within a related dithiaspirane-bridged decaammine system.⁵ The results in water with sulfate dianion, on the other hand, are qualitatively similar to those obtained for **1** with M^{n+} ; i.e., E^{MMCT} increases sharply and then decreases as the electrolyte concentration increases. Although we have not examined reaction 11 in the same detail

(22) Water was chosen to facilitate electrolyte solubility. Unfortunately, the addition of PF_6^- -containing electrolytes to aqueous solutions of the decaammine complex causes precipitation of the complex.

(23) If E^{MMCT} vs the Guntelberg parameter is not the appropriate function for extrapolation to zero ionic strength, then conclusions from a related study^{5b} involving the extrapolation perhaps also merit reevaluation. In particular, deductions concerning the magnitude of the "inner-shell" or vibrational component of the reorganization energy, as well as the functional dependence of the solvational component, might be worthy of reconsideration.

as the intervalence reactions of 1, we suggest that a similar explanation (stepwise ion pairing by SO_4^{2-}) is appropriate:



Intervalence transfer within the inherently unsymmetrical ionic assembly, $\text{SO}_4^{2-} \cdot (\text{NH}_3)_5\text{Ru}^{\text{III}}-4,4'\text{-bpy}-\text{Ru}^{\text{II}}(\text{NH}_3)_5^{5+}$, should occur at a higher energy than it does in either the unpaired species (lhs, eq 12a) or the doubly paired assembly (rhs, eq 12b) (cf. Figure 8). Predominance of the unsymmetrical assembly at low to intermediate Na_2SO_4 concentrations would account for the observed blue shift in E^{MMCT} over the same concentration range (Figure 11). (Note that the pattern of energy shifts here cannot be explained simply on the basis of nonspecific ionic atmosphere reorganizational effects.)

It is tempting, on the basis of the results with SO_4^{2-} , to offer a similar explanation for the systematic blue shifts with added $\text{TBA}^+\text{PF}_6^-$ (Figure 10); however, the lack of an eventual red shift (within the available electrolyte concentration range) requires an explanation. We speculatively suggest either (a) that anion pairing (or higher order association) occurs only with the $\{(\text{NH}_3)_5\text{Ru}^{\text{III}}\}^{3+}$ fragment (cf. eq 1) or more probably (b) that PF_6^- association with $\{\text{Ru}^{\text{II}}(\text{NH}_3)_5\}^{2+}$ begins before (multiple) association with the 3+ site is complete (i.e., species such as $\text{PF}_6^- \cdot (\text{NH}_3)_5\text{Ru}^{\text{II}}-4,4'\text{-bpy}-\text{Ru}^{\text{III}}(\text{NH}_3)_5^{5+} \cdot (\text{PF}_6^-)_2$ etc. may exist). Ultimately a total of five singly-charged anions should be capable of associating with the decaammine complex. Clearly, however, association with the 3+ site will be electrostatically favored; to the extent that it is favored, structural and energetic asymmetry effects will necessarily exist.

If either explanation is correct, then the key parameters for characterizing the concentration-dependent energy effects are the electrolyte anion/metal complex cation association constants and activities. In the existing literature on intervalence salt effects, alternatives such as "Guntelberg parameters" (which approximately relate ionic activities to ionic strengths) have sometimes been advocated;⁵ their use can be justified on a fundamental basis, however, only if nonspecific effects (e.g. ionic atmosphere reorganization) dominate the energetics.

Assuming that a specific, ion-pairing type explanation indeed is fully appropriate for reaction 11 (Figures 10 and 11), and assuming that a similar explanation is appropriate for the dithiaspirane-bridged analog studied by Lewis and co-workers, then the present studies additionally suggest a relatively simple explanation for some otherwise puzzling observations for the latter.^{5c} Specifically, they suggest an explanation for the apparent dependence of E^{MMCT} for $(\text{NH}_3)_6\text{Ru}^{\text{III}}-\text{dithiaspirane}-\text{Ru}^{\text{II}}(\text{NH}_3)_5^{5+}$ (in DMSO) on the identity of the oxidant employed to generate the mixed-valence (5+) complex from the 4+ form. Lewis and co-workers found that E^{MMCT} progressively increased as the oxidant changed from $[\text{Ru}(2,2'\text{-bpy})_2(\text{CN})_2](\text{NO}_3)$ to $[\text{Ru}(2,2'\text{-bpy})(\text{PPh}_3)\text{Cl}](\text{NO}_3)_2$ to $[\text{Ru}(2,2'\text{-bpy})_2(\text{pyridine})_2](\text{NO}_3)_3$ and finally to $[\text{Ru}(2,2'\text{-bpy})_3](\text{NO}_3)_3$.^{5c} They further noted that this is approximately the order of oxidizing strengths and suggested that this might be consistent with a special (unknown) "cofactor" role for the oxidant in the optical ET process.

A simpler explanation centers on the progressive increase in total anion concentration as the oxidant charge (and hence number of accompanying anions) is increased. To appreciate

why this could be significant, it is important to recall that intervalence bands are extremely weak in dithiaspirane-bridged systems.⁵ Consequently, relatively high concentrations of diruthenium complex (and oxidant) are needed in order to observe the bands. The range of concentrations used in the variable oxidant study was not specified. In a related study, however, the lowest ionic strength employed (in DMSO) was ~ 0.15 M.^{5b} Given the oxidant (ceric ammonium nitrate), the lowest diruthenium concentration apparently was about 3.3 mM. If a similar minimum diruthenium concentration was employed in the variable oxidant study, the total anion concentration would have varied between roughly 16 and 23 mM (as the identity of the oxidant was changed). (Obviously, if the minimum chromophore concentration were higher, then even larger absolute changes in anion concentration would have resulted.) From Figure 10, total anion concentration variations from 16 to 23 mM (or larger) would be sufficient to induce detectable intervalence energy shifts (with higher energies accompanying higher anion concentrations). Indeed, Figures 10 and 11 would predict—for any fixed mixed-valence ion concentration—that E^{MMCT} would change with oxidant identity in the order $[\text{Ru}(2,2'\text{-bpy})_2(\text{CN})_2](\text{NO}_3) < [\text{Ru}(2,2'\text{-bpy})(\text{PPh}_3)\text{Cl}](\text{NO}_3)_2 < [\text{Ru}(2,2'\text{-bpy})_2(\text{pyridine})_2](\text{NO}_3)_3 \approx [\text{Ru}(2,2'\text{-bpy})_3](\text{NO}_3)_3$. Note that this is the order reported in the optical experiments.^{5c} Finally, in the optical studies, extrapolation of intervalence energy measurements to zero ionic strength was claimed. This would seemingly negate the ion-pairing explanation (and, for that matter, any "cofactor" explanation involving finite cofactor/mixed-valence-ion association constants). The reliability of any extrapolation depends critically, however, on the validity of the function used for extrapolation. As we have noted above, the appropriate function cannot be E^{MMCT} vs the Guntelberg parameter (i.e., $\mu^{1/2}/(1 + \mu^{1/2})$, where μ is the ionic strength), if the origin of the energy effect is unsymmetrical ionic association. (Nor can it be the correct function if cationic cofactor/cationic mixed-valence-ion association is the origin.) We prefer, therefore, an explanation that emphasizes *specific* ionic association effects and symmetry reduction effects.

Conclusions

A model that considers the energetic consequences of stepwise ion pairing can account, at least qualitatively, for the unusual optical intervalence absorption response of $(\text{NC})_5\text{Fe}^{\text{III}}-\text{BPE}-\text{Fe}^{\text{II}}(\text{CN})_5^{5-}$ in variable ionic strength solutions of LaCl_3 , CaCl_2 , and NaCl . The model also can account for the unusual optical intervalence properties of $(\text{NH}_3)_5\text{Ru}^{\text{III}}-4,4'\text{-bpy}-\text{Ru}^{\text{II}}(\text{NH}_3)_5^{5+}$ in aqueous Na_2SO_4 solutions. The experiments and associated model illustrate the important role that ion-pairing-induced symmetry reduction and subsequent restoration can play in optical electron transfer processes. We speculatively suggest the symmetry reduction effect described here is also responsible for the previously reported^{5c} chemical oxidant dependence of E^{MMCT} for a dithiaspirane-bridged decaamminediruthenium system.

Acknowledgment. We thank the U.S. Department of Energy, Office of Energy Research, Division of Chemical Sciences, for support of this work (Grant No. DE-FG02-87ER13808). J.T.H. also acknowledges support from the Henry and Camille Dreyfus Foundation (Teacher-Scholar Award, 1991–6).